

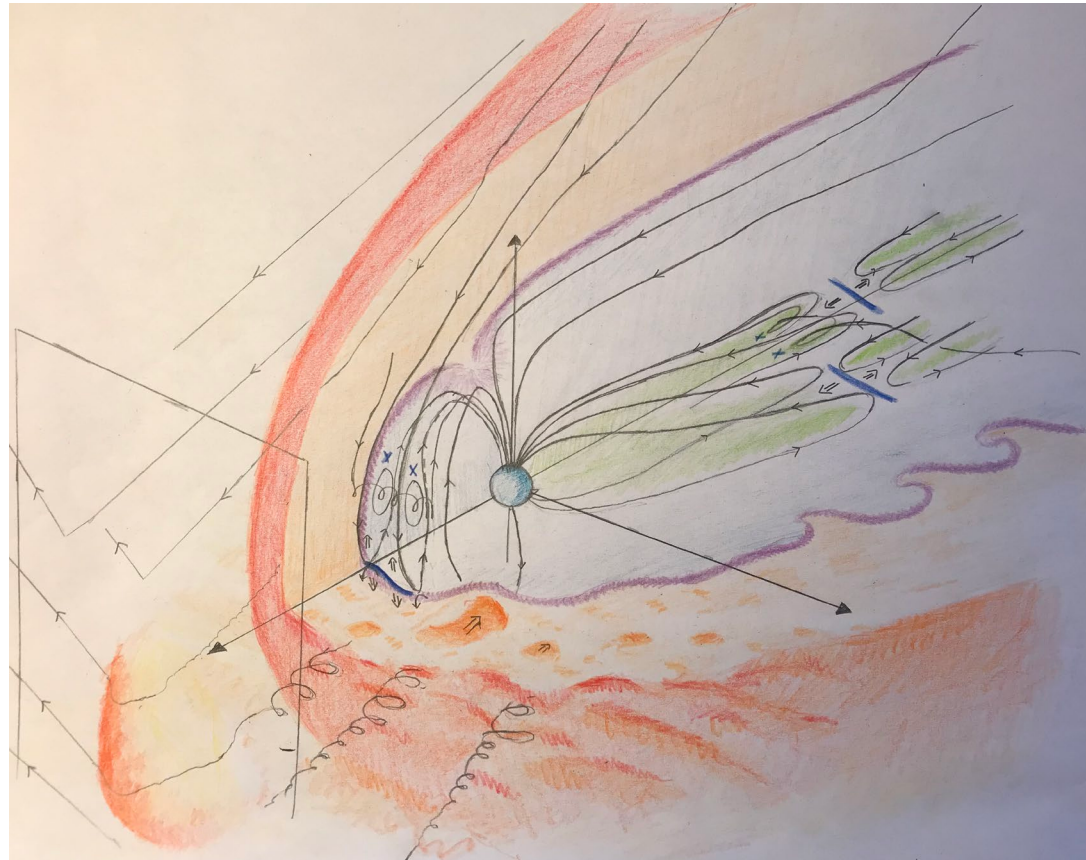
The Bow Shock and The Foreshock

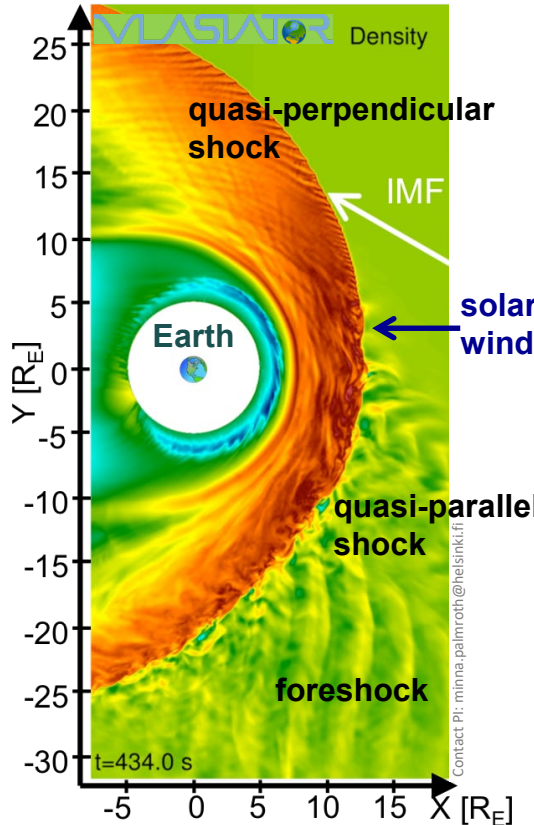
Heli Hietala

Thank you: International Space Science Institute team 465 “Foreshocks Across the Heliosphere”,
Imperial Magnetosphere team, Vlasiator team, Univ. Turku SRL, PROSPERO team

Why do we care? about the bow shock and the foreshock

- Process the solar wind before it interacts with the magnetosphere
- Generate structures
- Accelerate particles
- Host fundamental plasma physics processes

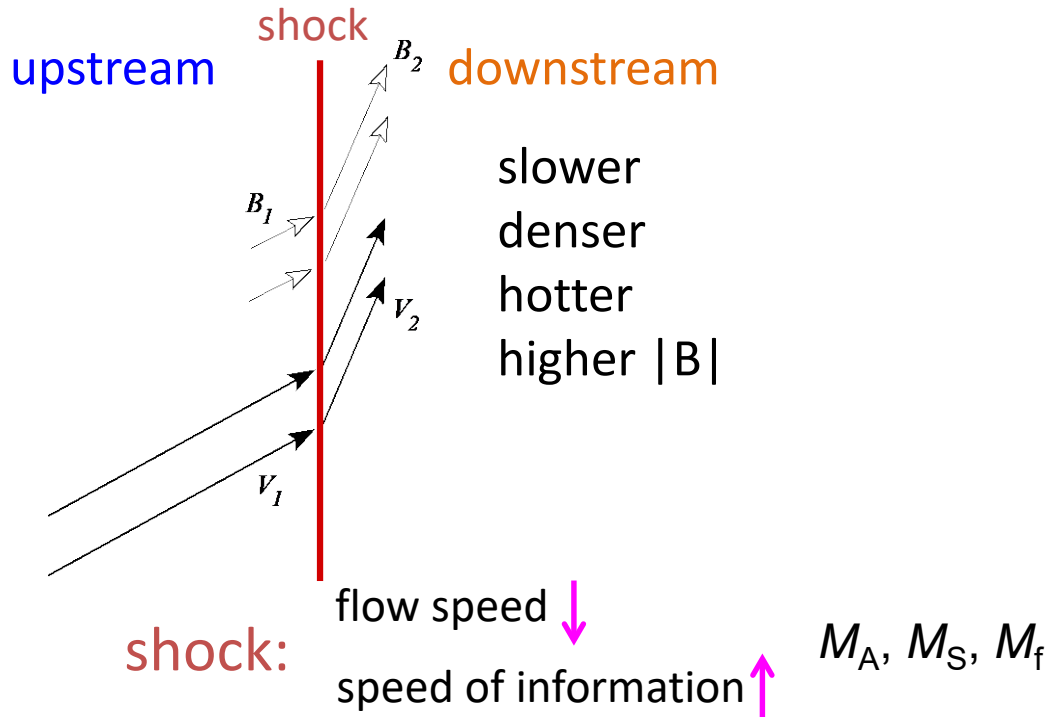




Outline: from large to small

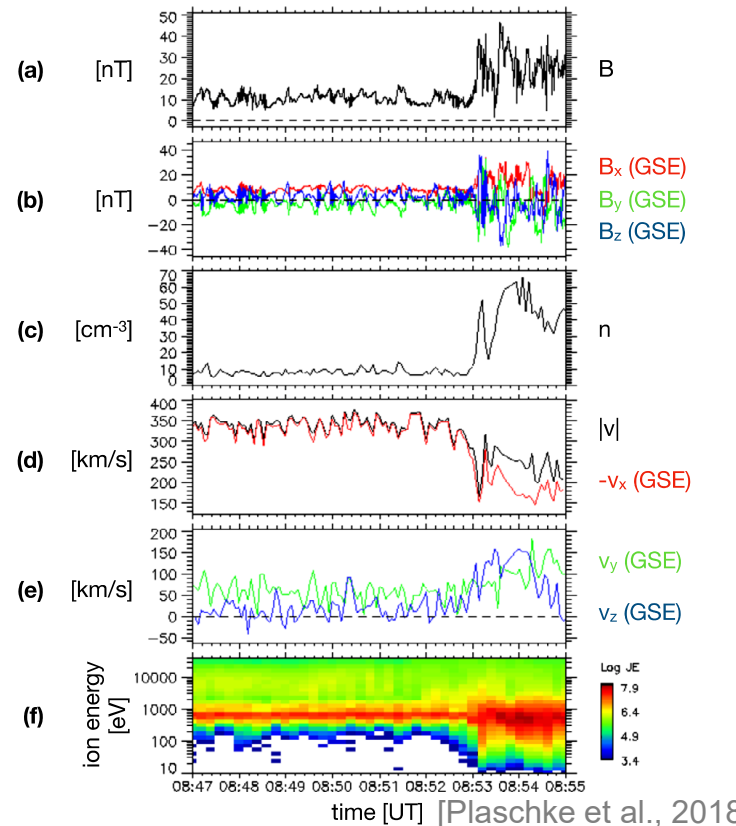
1. What is a shock? ($\sim 20 R_E$)
2. Shock obliquity:
quasi-perpendicular and quasi-parallel ($\sim 10 R_E$)
Electron and ion foreshocks
3. Foreshock structures
 1. Driven foreshock structures ($2-10 R_E$)
 2. Intrinsic foreshock structures ($1 R_E$)
4. Fine structure (10-100 km)
Perpendicular shock ripples
Reconnection within the shock front
5. What next?

1 What is a space plasma shock?

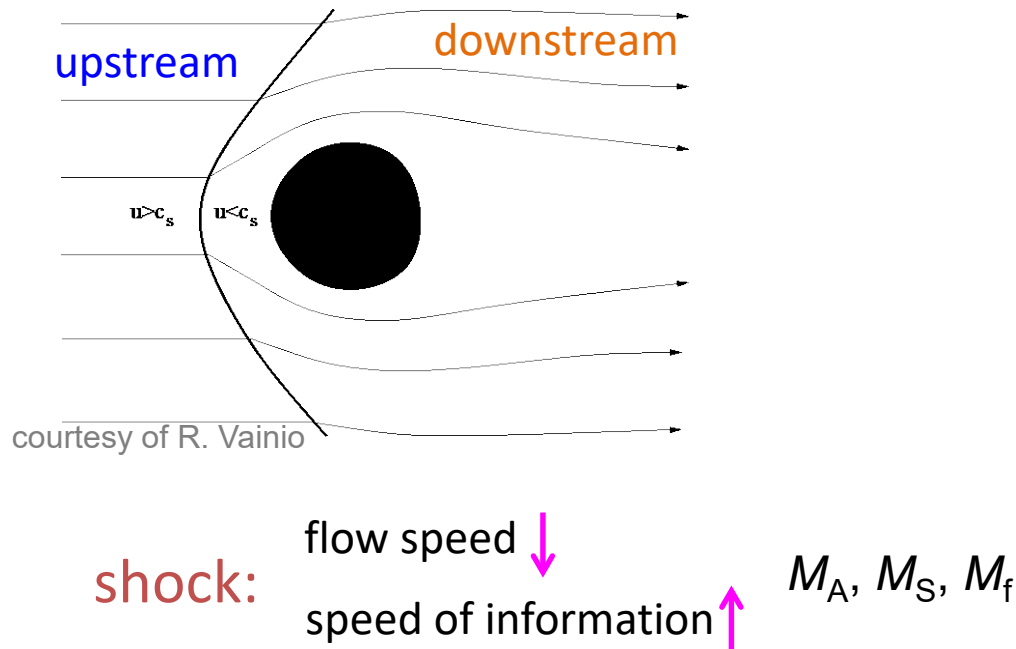


11 May 2020

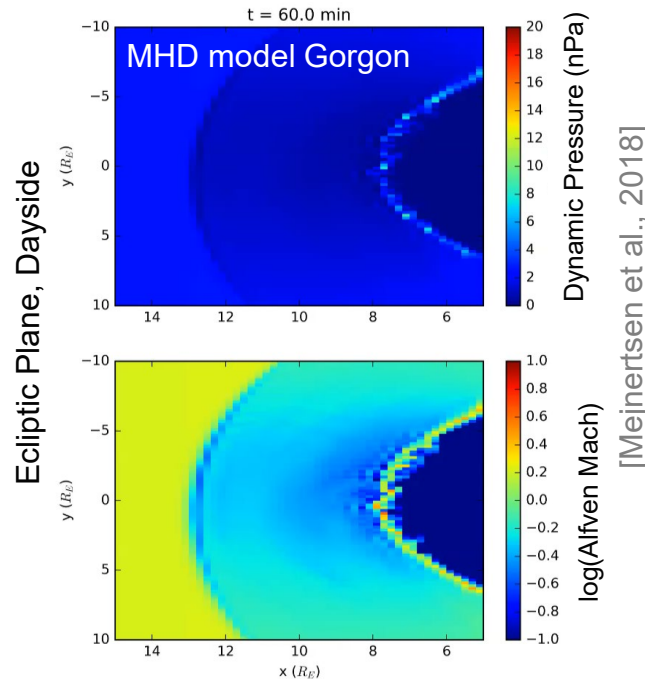
Cluster 1 – 18 February 2002



1 Magnetosphere as an obstacle



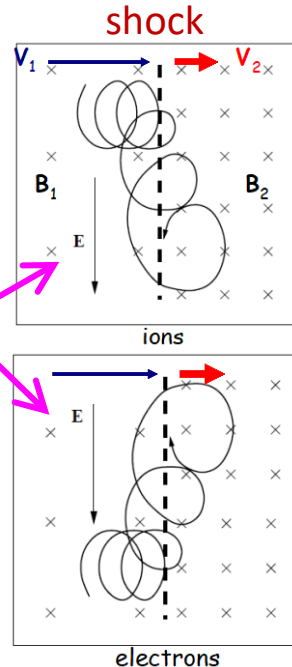
Bow shock position varies
mainly with solar wind dynamic pressure



1 Particle acceleration 101

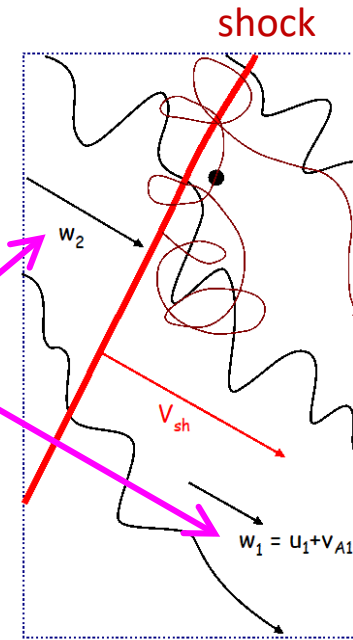
Shock Drift Acceleration

particles gain energy by drifting along/against the convective electric field



Diffusive Shock Acceleration

multiple interactions with waves upstream and downstream lead to multiple shock crossings



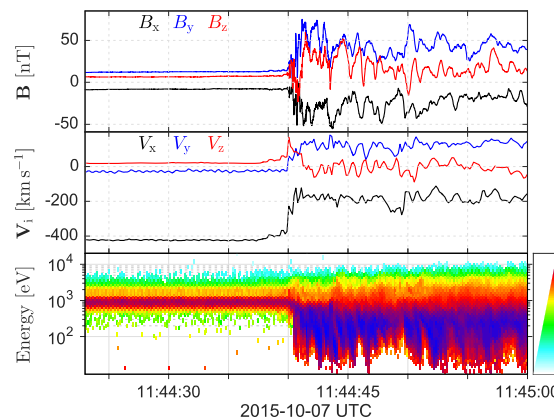
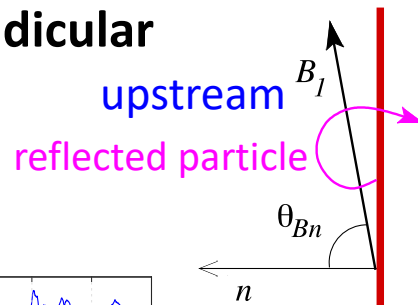
figures: R. Vainio

Earth's bow shock is relatively small:
Under typical solar wind conditions and without an interplanetary seed population, it does not accelerate ions above 200-330 keV

[Meziane et al., 2002]

2 Magnetic field orientation: shock obliquity

quasi-perpendicular



[Johlander, et al., 2016b]

upstream

B_I

upstream

B_I

shock

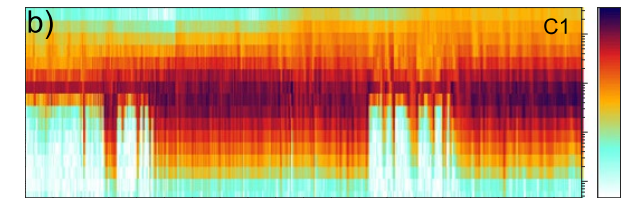
quasi-parallel

reflected particle

n

θ_{Bn}

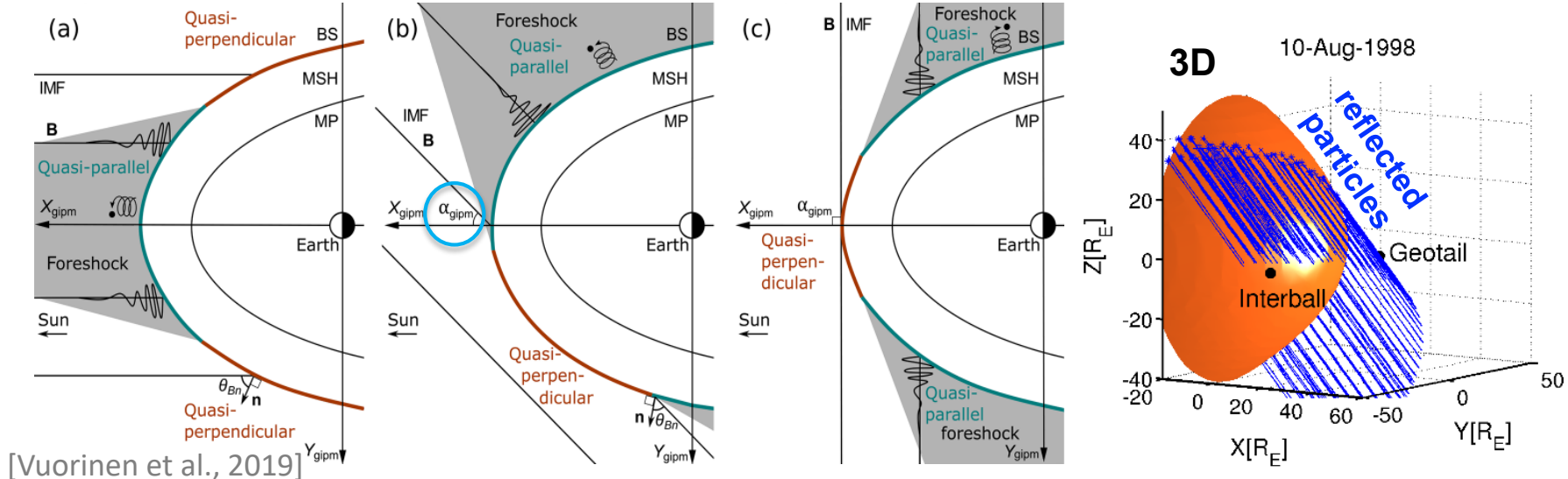
oblique



[Johlander et al., 2016a]

2 Curved bow shock

quasi-perpendicular and quasi-parallel regions coexist



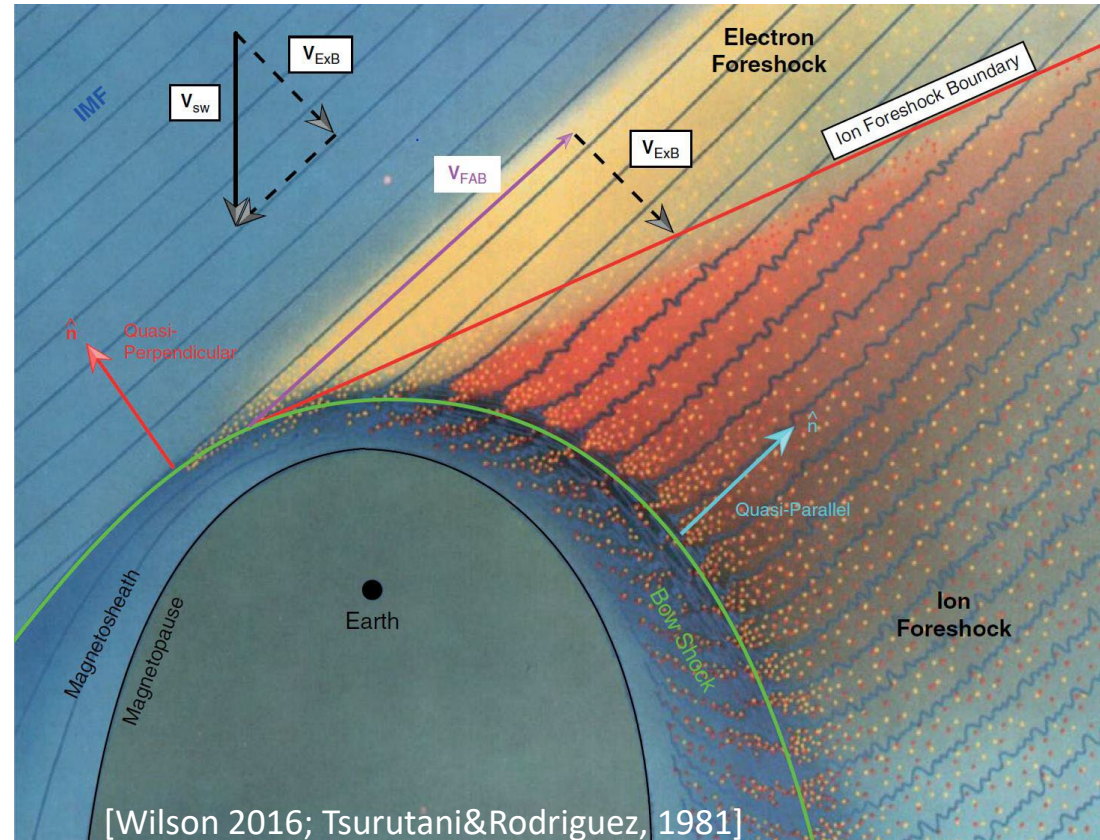
[Vuorinen et al., 2019]

key quantity: IMF cone-angle $\alpha = \cos\left(\frac{B_x}{B}\right) \in [0^\circ, 90^\circ]$

(also for the magnetospheric effects of shock dynamics)

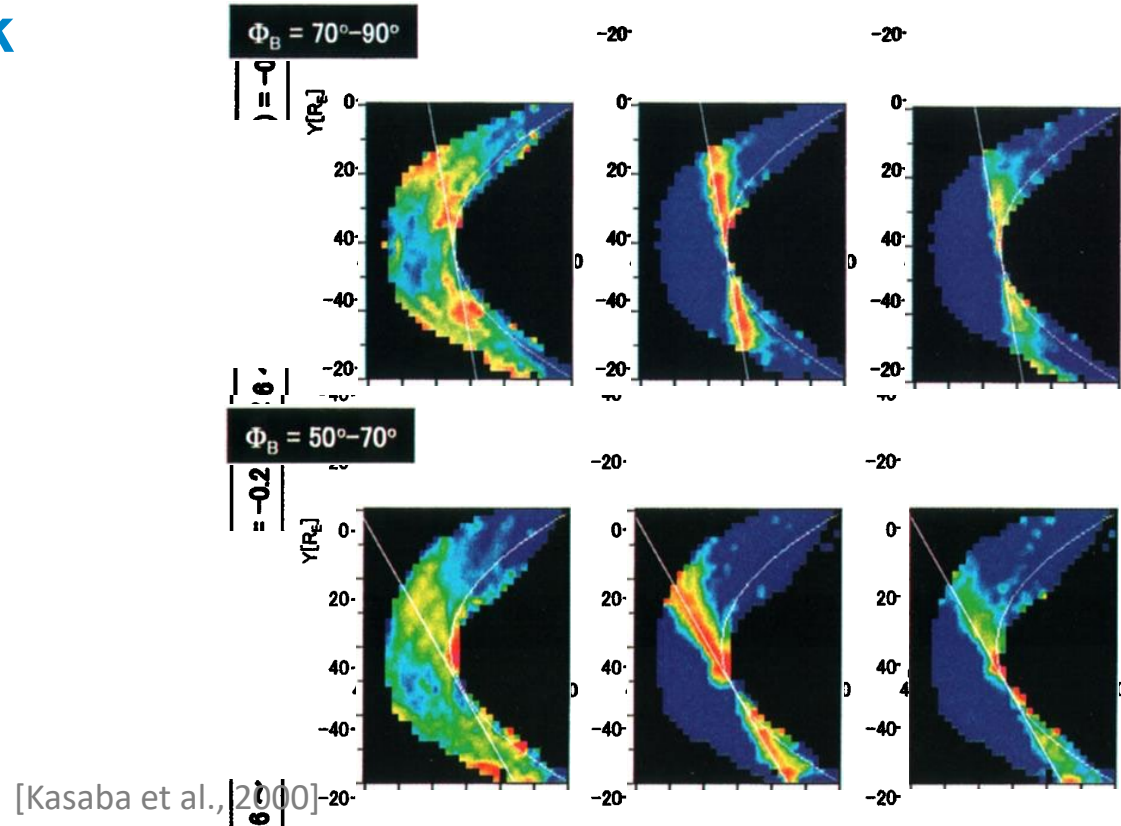
2 Foreshock and velocity filter effect

- Foreshock = region upstream of and magnetically connected to the shock and filled with reflected particles and associated instabilities/waves
- ($E \times B$)-drift velocity is the same for all particles
 - fastest reflected particles seen closest to the tangent field line
 - separation to electron and ion foreshocks
 - particles reflected at a higher θ_{Bn} will advect to and modify the shock front at a lower θ_{Bn}

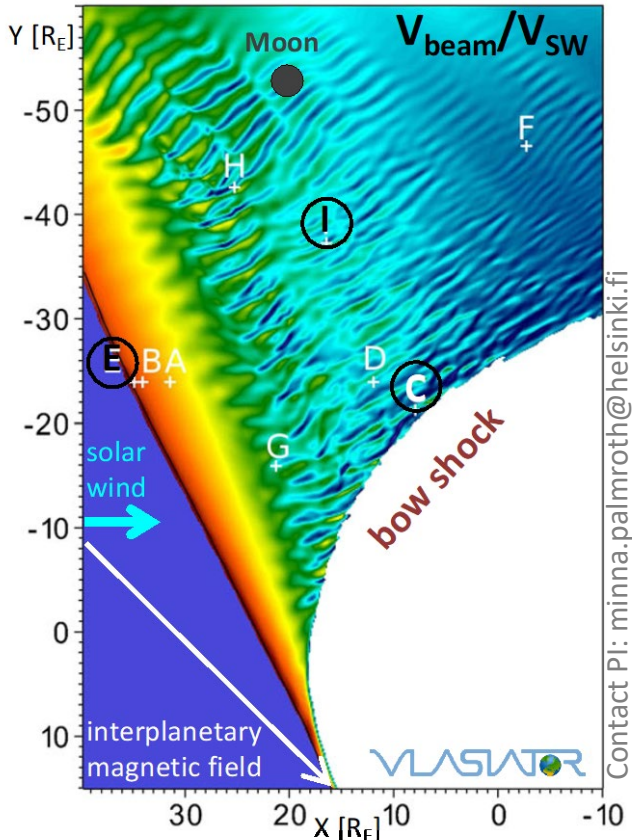


2 Electron foreshock

- Electron beams (>1 keV) generate Langmuir waves at the electron plasma frequency, which convert to radio emission at twice the electron plasma frequency
- ISEE-1, Wind, Cluster measurements
- Examples of statistical maps built from Geotail observations
[Kasaba et al., 2000]

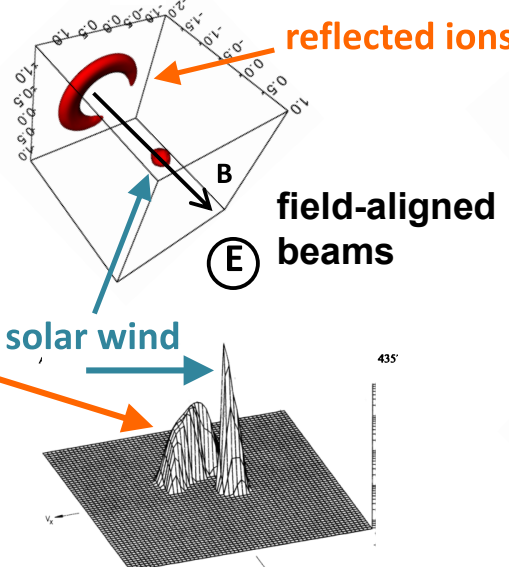


[Kasaba et al., 2000]

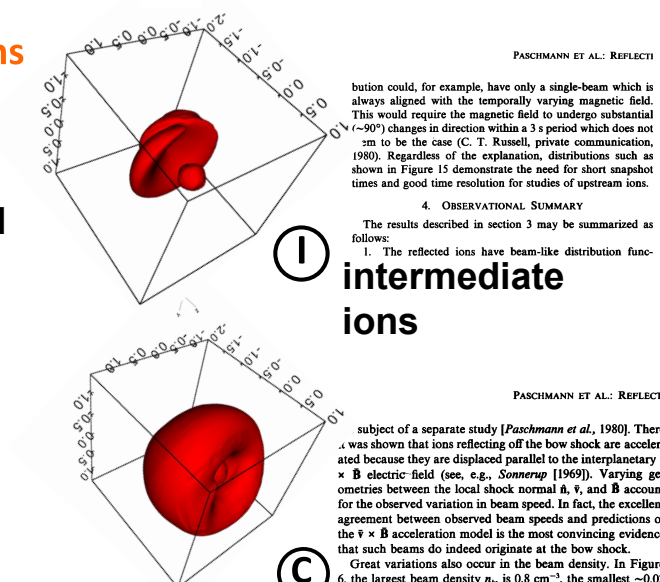


2 Ion foreshock: distribution functions

hybrid-Vlasov simulations and ISEE observations

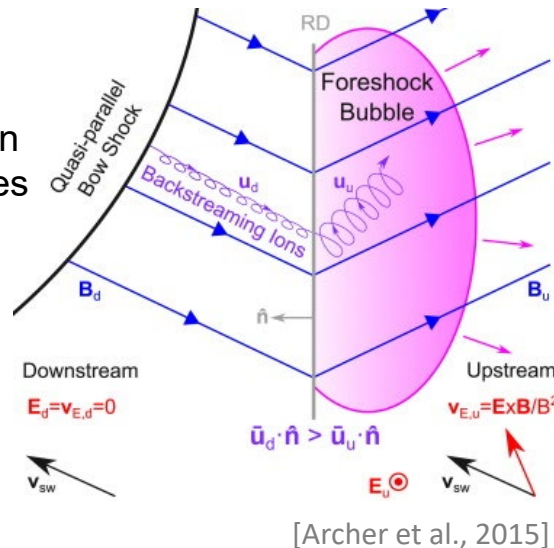


[Kempf et al., 2015; Paschmann et al., 1981]



3.1 Driven foreshock structures: foreshock bubbles

- what:** a hot core of low density, low magnetic field, with an upstream shock
- driven by** rotational and thin tangential IMF discontinuities [e.g., Liu et al., 2015]
- size $> 3 R_E$**
simulations indicate up to the same size as the whole foreshock [Omidi et al., 2010; Liu et al., 2019]
- occurrence rate** ~1/day under favorable high solar wind speed conditions [Turner et al., 2013]

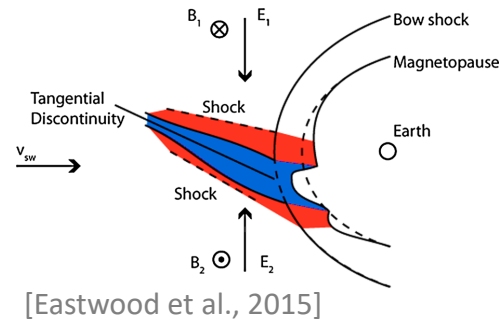


[Archer et al., 2015]

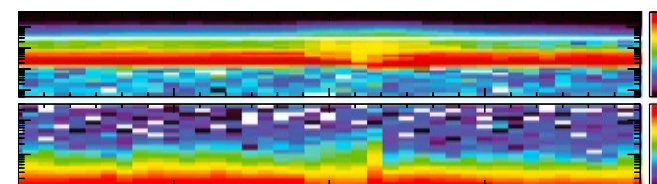
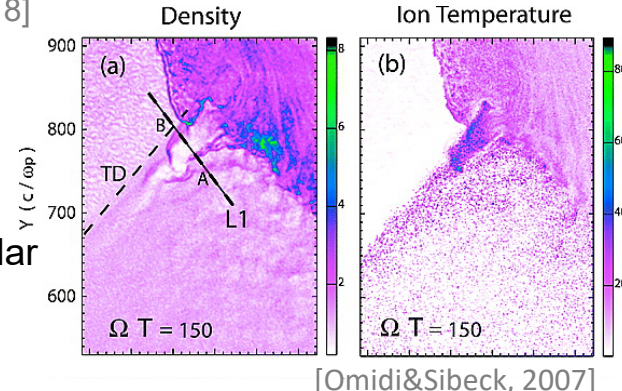
[Turner et al., 2013]

3.1 Driven foreshock structures: hot flow anomalies

- **what:** suprathermal ions channeled upstream at the **intersection** of a discontinuity with the bow shock, with compressions at its edges
- AMPTE-UKS:
Schwartz et al. [1985]
- MMS: Schwartz et al. [2018]
- **size a few R_E**
increases as it travels across the shock
- **occurrence rate** $\sim 2/h$
under favorable high solar wind speed conditions
[Turner et al., 2013]



[Eastwood et al., 2015]



3.1 Driven foreshock structures: key effects

Particle Acceleration

- **Transients with hot, low density cores and compressional boundaries**
 - leading shock reflects solar wind ions (secondary foreshock) [Liu et al., 2016]
 - occasional ion acceleration [Liu et al., 2017a; Turner et al., 2018]
 - energized ions leak out of the core [Liu et al., 2017b]
 - **electrons almost always energized, up to 100s of keVs** [Wilson et al., 2016, Liu et al., 2017a,c]

Magnetospheric Response

Foreshock Bubble

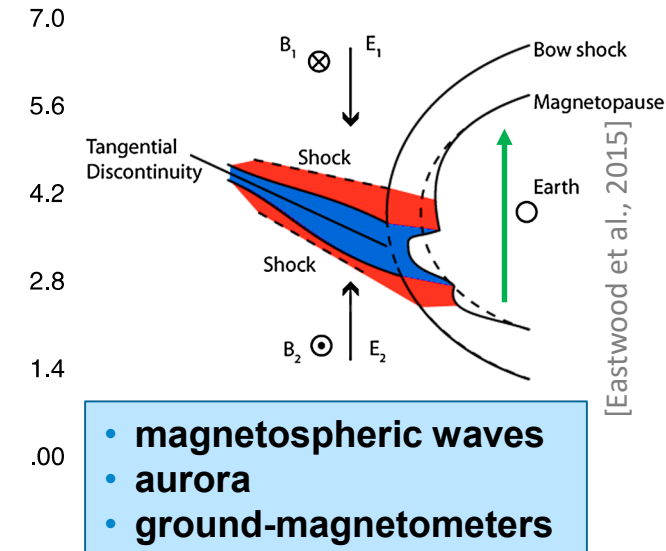
almost global out-in motion



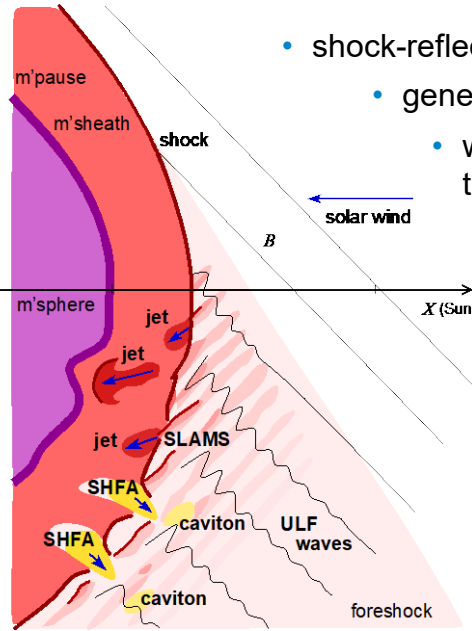
[Turner et al., 2013]

Hot Flow Anomaly

a sweeping bulge



3.2 Intrinsic foreshock structures: overview



- shock-reflected ions stream against the solar wind
 - generate waves ($\sim 30s$; $\sim 1R_E$)
 - waves are advected back towards the shock
- waves undergo nonlinear interactions with themselves, the ions, and locally generated waves, generating structures:
 - troughs/depressions
 - **cavitons**
 - **spontaneous hot flow anomalies**
- peaks/enhancements
 - **shocklets**
 - **short large amplitude magnetic structures (SLAMS)**

3.2 Where it starts: waves

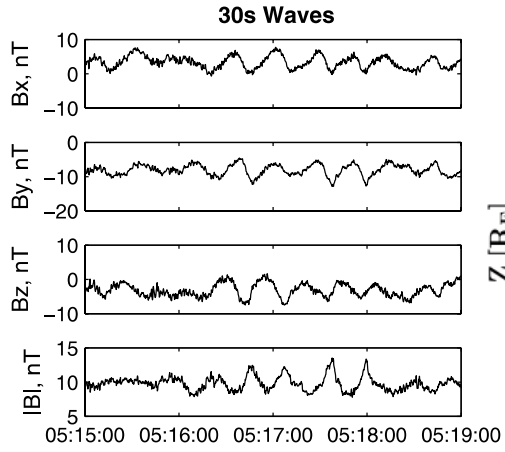
- focus:** sunward propagating fast magnetosonic waves
- generated by** right-hand ion-beam instability between SW and reflected ions
- period** depends on IMF strength and orientation:

$$\omega_{sc} = \frac{qB}{m} \frac{\cos \theta_B}{\cos \theta_{nx}} \frac{\cos \theta_{Bn}}{\cos \theta_{nx}}$$

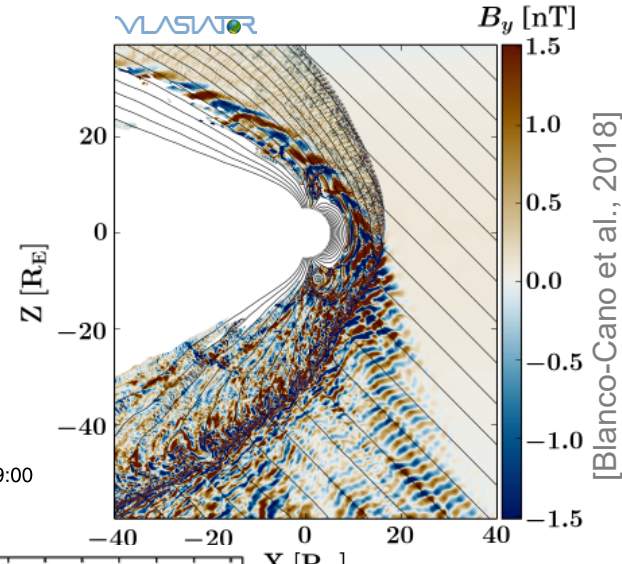
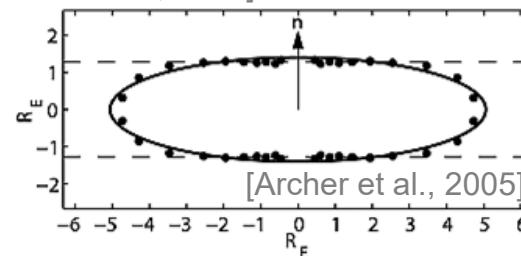
[Takahashi et al., 1984; Le&Russell, 1996]

~30s period at Earth; ~1 R_E wavelength

- large amplitude $|\delta\mathbf{B}|/B \sim 1$
- \mathbf{k} deflected from \mathbf{B} $\sim 20^\circ$ due to refraction by spatially varying suprathermal ions
- convected by the solar wind towards the shock, modify it, and transmit into the magnetosphere



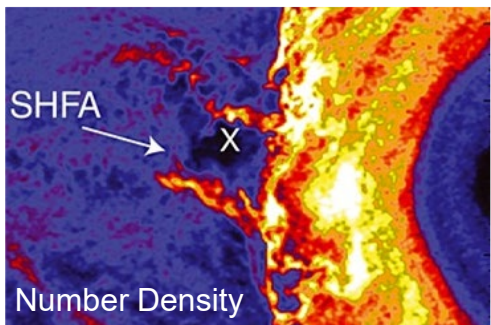
[Eastwood et al., 2005]



Recent review:
[Wilson 2016]

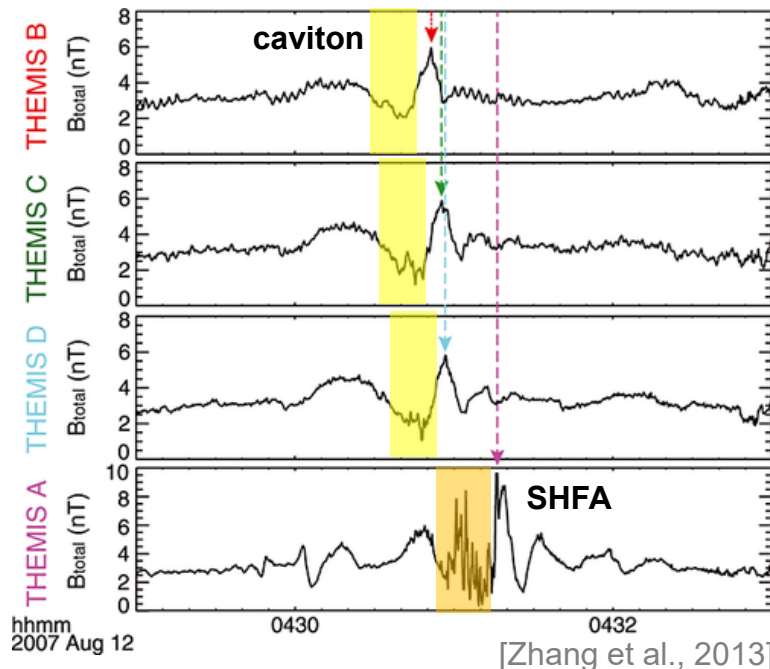
3.2 Troughs: cavitons and spontaneous hot flow anomalies

- **cavitons:** depressions of n and B, but no T increase, with “shoulders” at outer edges
- **where:** deep in the ion foreshock, surrounded by waves [Kajdic et al., 2017]
- **form by** interaction of parallel and obliquely propagating waves [Blanco-Cano et al., 2009]
- **Spontaneous Hot Flow Anomalies:** decrease in n and B, with increase in T
- **form from** cavitons [Zhang et al., 2013]



[Omidi et al., 2013]

- **size $\sim 1 R_E$**
same as 30s waves
- **effects:** modify (weaken)
the bow shock



[Zhang et al., 2013]

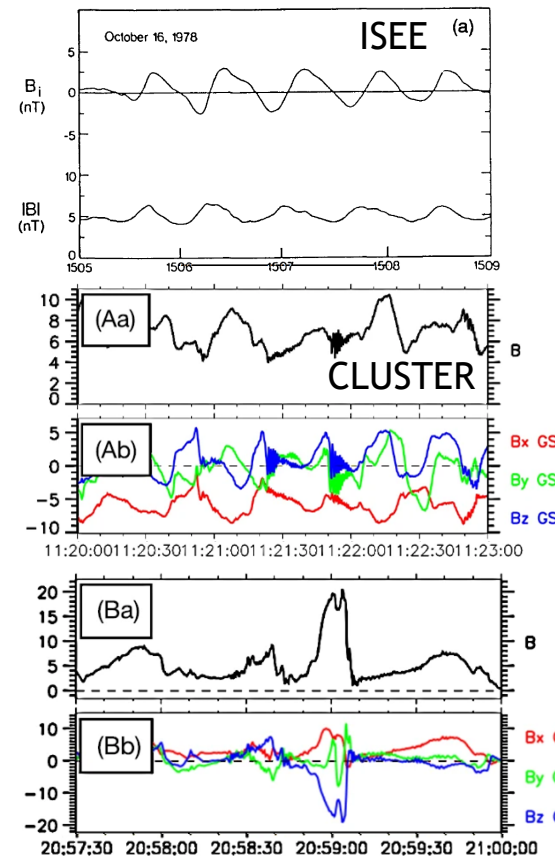
3.2 Peaks: shocklets and SLAMS

- “**30s waves**”: fast magnetosonic waves $|\delta B|/B_0 \sim 1$
- **shocklets**: steepened waves, associated with whistler wave packets and diffuse backstreaming ion distributions, $1 \lesssim |\delta B|/B_0 \lesssim 2$ [e.g., Hoppe et al., 1981]
- **where**: close to the bow shock
- **size $\sim 1 R_E$** ($\sim 30s$) [e.g., Le and Russell, 1994]
- **Short Large Amplitude Magnetic Structures (SLAMS)**: fast mode pulsations, monolithic, $|\delta B|/B_0 > 2$ (up to 10)
- **where**: close to the bow shock (they are the shock)
- **size > 1000 km** [Lucek et al., 2004; 2008]
- **importance**: ion energization by reflection and trapping slow down the incoming flow
“building blocks” of the quasi-parallel shock
[e.g., Schwartz et al., 1991; 1992; Johlander et al., 2016a]

“30s waves”

shocklets

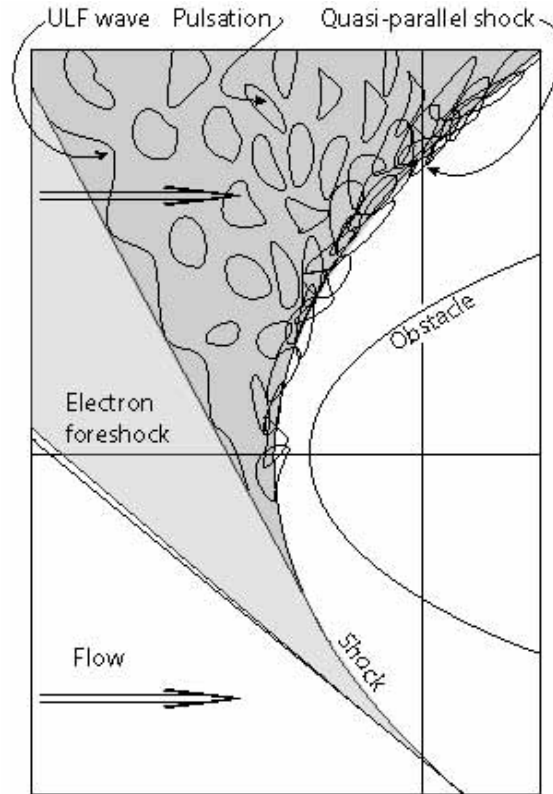
SLAMS



[Hoppe et al., 1983]

[Plaschke et al., 2018]

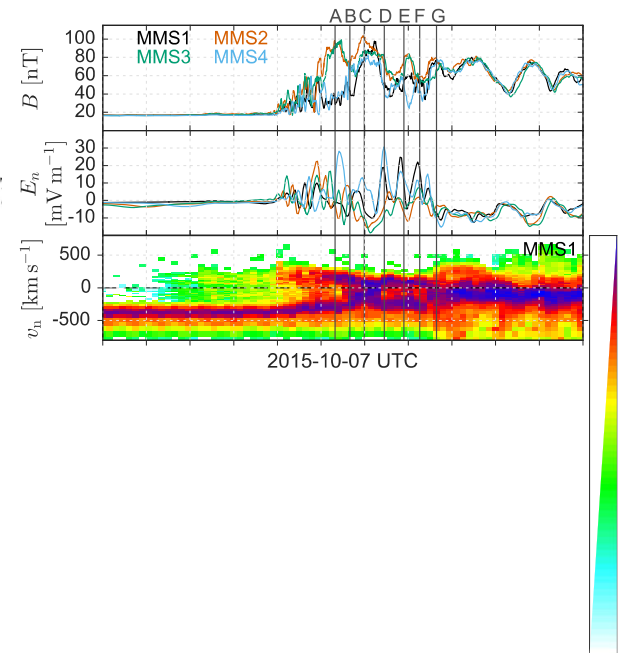
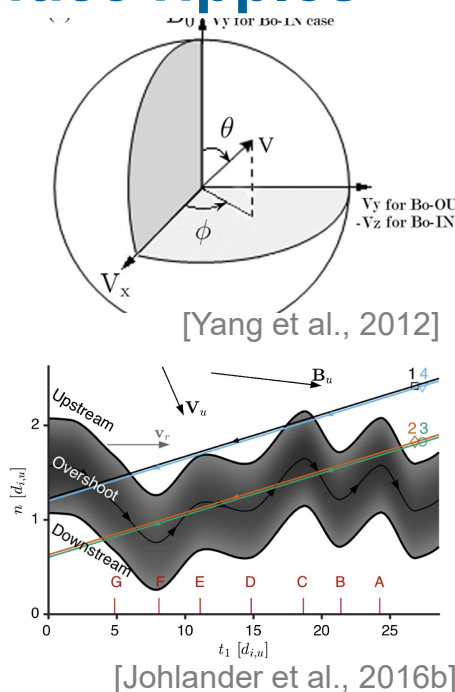
From meso-scale to fine structures



[Treumann&Jaroschek, 2008]

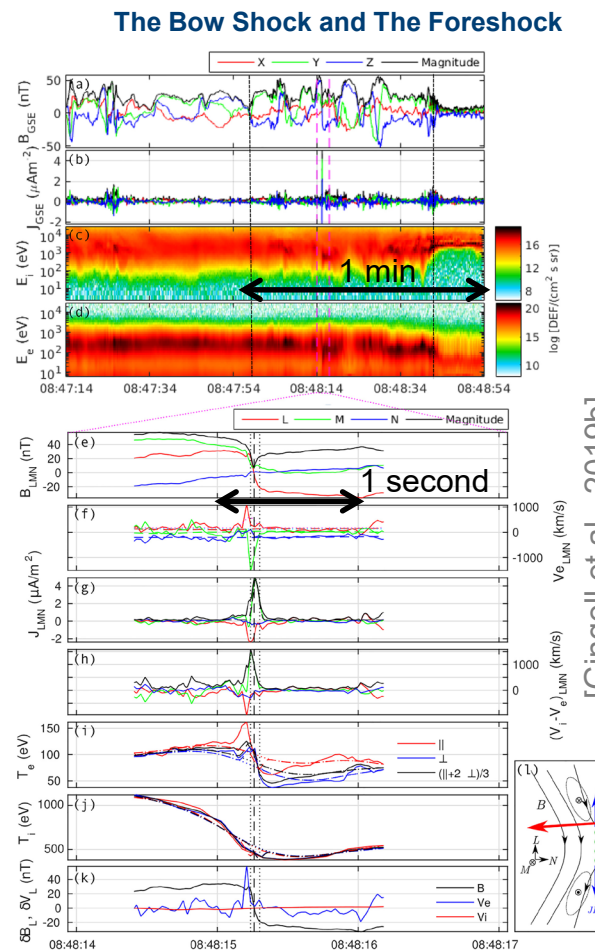
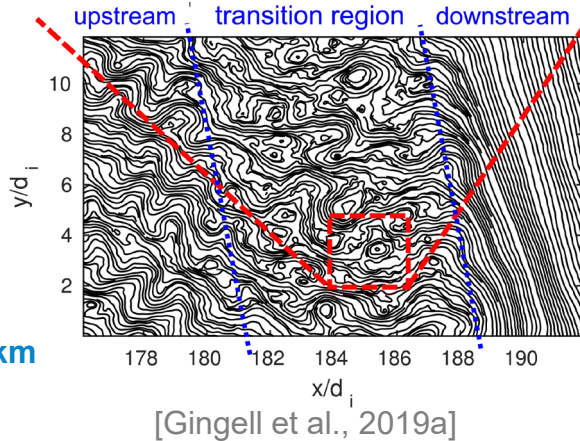
4 Fine structures: quasi-perp shock surface ripples

- Shock non-stationarity: ripples and reformation
- Affects electron acceleration and ion reflection
- Simulation predictions [e.g., Lowe&Burgess 2003]
- Quantitative observations [Johlander et al., 2016b]
 - ripple wavelength $\sim 4 d_{iu} \sim 175$ km
 - ripple amplitude $\sim 0.25 d_{iu} \sim 10$ km



4 Fine structure: reconnection within the shock front

- First observed at oblique and quasi-parallel geometries
[Wang et al., 2019;
Gingell et al., 2019a]
- Statistical observations
[Gingell et al., 2019b]
 - present for all shock obliquities
 - current sheet widths $\lesssim 10 d_e \sim 8\text{ km}$
 - typically feature electron-only reconnection
 - primary consequence:** relaxing magnetic topology (not heating)
- Simulations
[Bohdan et al., 2017; Gingell et al., 2017; Matsumoto et al., 2015]



5 What next: comparative planetary foreshock studies

A challenge for our understanding Under-explored datasets Different processes

“30s wave” scaling

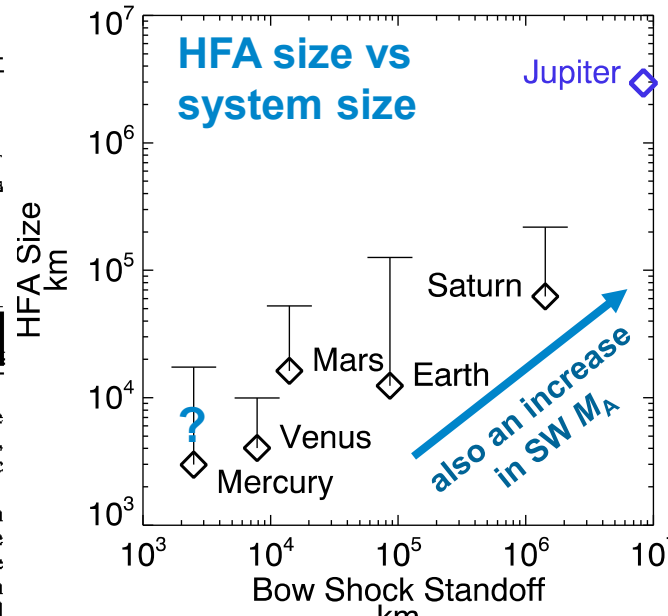
41

- 18. Manley, J. L. *J. molec. Biol.* **125**, 449–466 (1978).
- 19. Steege, D. A. *Proc. natn. Acad. Sci. U.S.A.* **74**, 4163–4167 (1977).
- 20. Napoli, C., Gold, L. & Swobelin Singer, B. *J. molec. Biol.* **149**, 433–449 (1981).
- 21. Atkins, J. F., Gesteland, R. F., Reid, B. R. & Anderson, C. W. *Cell* **18**, 1119–1131 (1979).
- 22. De Mars Cody, J. & Conway, T. W. *J. Viro.* **37**, 813–820 (1981).
- 23. Gorini, L. in *Ribosomes* (eds Nomura, M., Tissières, A. & Lengyel, P.) 791–803 (Cold Spring Harbor Monogr. Ser., 1974).
- 24. Sugiyama, T., Stone, H. & Nakada, D. *J. molec. Biol.* **42**, 97 (1969).
- 25. Maxam, A. & Gilbert, W. *Proc. natn. Acad. Sci. U.S.A.* **74**, 560–564 (1977).
- 26. Sander, F. et al. *Nature* **265**, 687–595 (1977).
- 27. Godson, G. N., Barrell, B. G., Staden, R. & Fiddes, J. *Nature* **276**, 236–247 (1978).

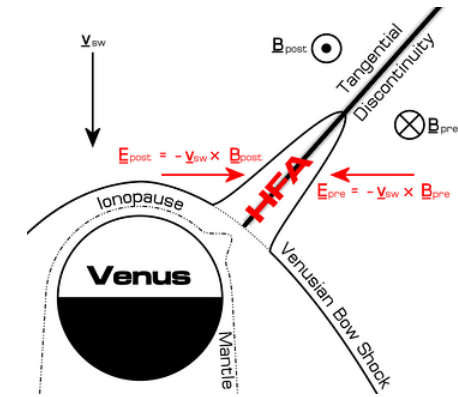
ONATURE

the observations⁹. These waves have been of interest for some time, partially because of their role in the foreshock structure, but also because of their apparent connection with geomagnetic pulsations of the same frequency.

The relationships between upstream conditions and pulsation character have been investigated on the hypothesis that the upstream waves may be the ultimate source of at least some classes of pulsations. A linear relationship between pulsation frequency and the magnitude of interplanetary magnetic field has been found^{10,11}. Russell and Hoppe¹² recently verified that the same relationship that holds for ground data also holds for



[Valek et al., 2017; Uritsky et al., 2014]



[Collinson et al., 2012]

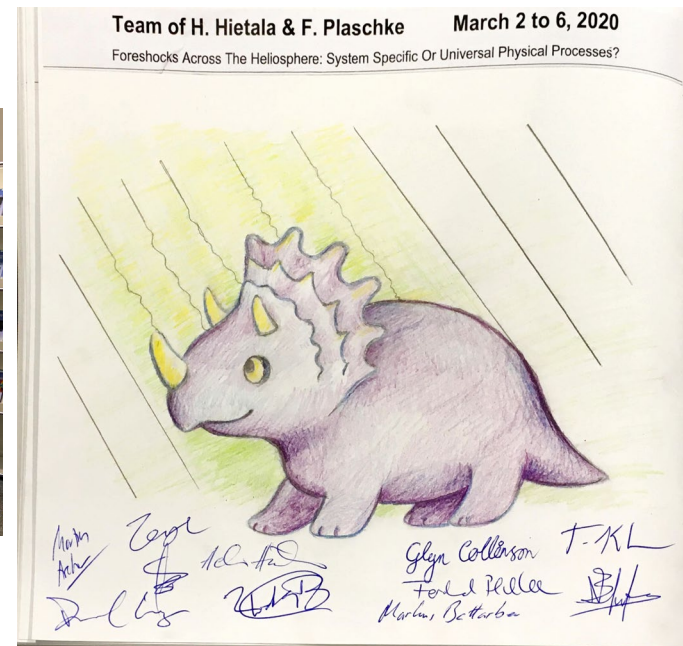
Foreshock-exosphere interactions

[Mazelle et al., 2018]

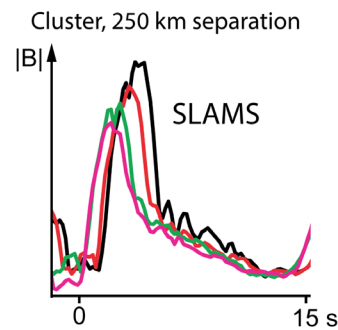
5 What next: comparative planetary foreshock studies

ISSI Team 465 Foreshocks Across the Heliosphere: System Specific or Universal Physical Processes?

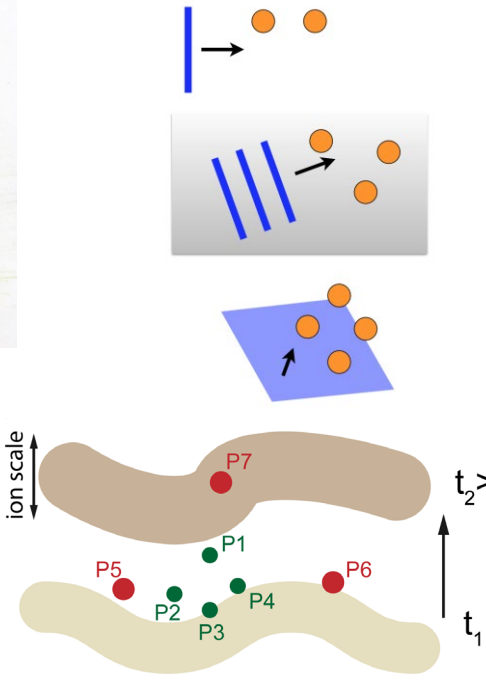
- Heli Hietala, UK
- Ferdinand Plaschke, Austria
- Martin Archer, UK
- Markus Battarbee, Finland
- Cesar Bertucci, Argentina
- Xochitl Blanco-Cano, Mexico
- Glyn Collinson, USA
- Tomas Karlsson, Sweden
- Terry Zixu Liu, USA
- David Long, UK
- Merav Opher, USA
- Savvas Raptis, Sweden
- Nick Sergis, Greece



5 What next for Earth: constellation mission



adapted from [Lucek et al., 2008]



1D motion: 2 spacecraft
e.g., ISEE 1-2

2D motion: 3 spacecraft

3D motion: 4 spacecraft
e.g., CLUSTER, MMS

*distinguish growth vs motion?
quantify non-planarity?
measure non-linear gradients?*

7 spacecraft

Thank you



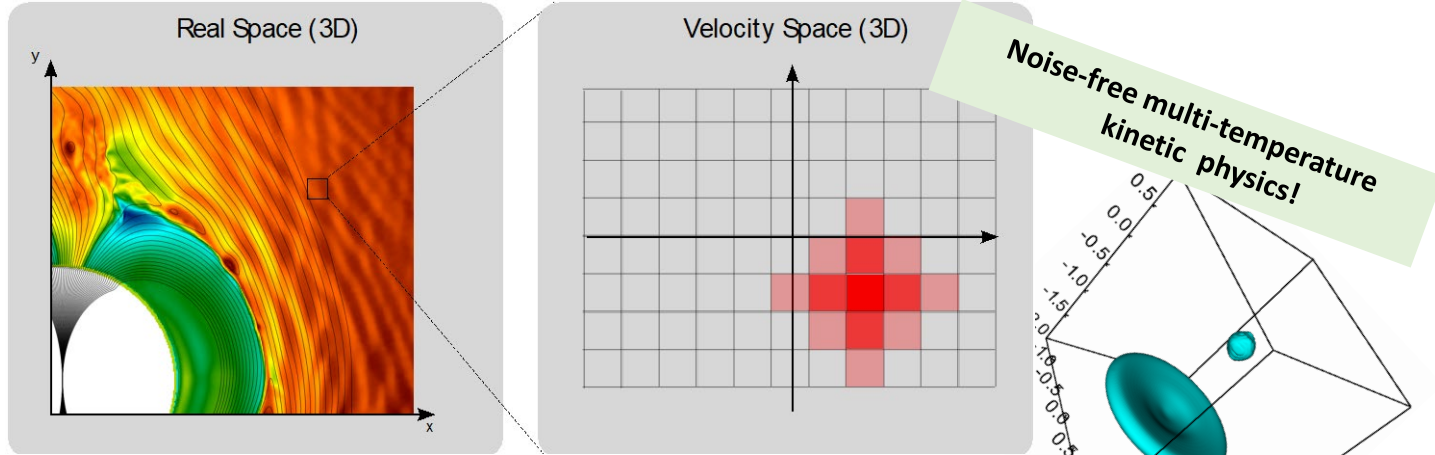
Backups



UNIVERSITY OF HELSINKI
FACULTY OF SCIENCE



- Ion-kinetic plasma physics
- Electrons are massless charge-neutralising fluid.



- Divide real space into grid cells
- Compute \mathbf{E} , \mathbf{B} fields in real space
- Each real space cell contains a 3D velocity space
- Self-consistent: In 6D, propagate distribution function using Vlasov equation
 - Couple back to ordinary space to update \mathbf{E} , \mathbf{B} field

More information: <http://physics.helsinki.fi/vlasiator>

Contact PI: Minna.Palmroth@helsinki.fi